JOURNAL OF AGRICULTURAL AND FOOD CHEMISTRY

Article

pubs.acs.org/JAFC

Hot-Spot Mapping of the Interactions between Chymosin and Bovine κ-Casein

Jesper Sørensen,[†,‡,§] David S. Palmer,[‡,#] and Birgit Schiøtt*[,†,‡]

[†]The Center for Insoluble Protein Structures (*in*SPIN) and the Interdisciplinary Nanoscience Center (*i*NANO) and [‡]Department of Chemistry, Aarhus University, Langelandsgade 140, DK-8000 Aarhus C, Denmark

Supporting Information

ABSTRACT: Chymosin is a commercially important enzyme in the manufacturing of cheese. Chymosin cleaves the milk protein κ-casein, which initiates the clotting process. Recently, it has been shown that camel chymosin has superior enzymatic properties toward cow's milk, compared to bovine chymosin. The two enzymes possess a high degree of homology. There are only minor differences in the binding cleft; hence, these must be important for binding the substrate. Models for the binding of a 16 amino acid fragment, consisting of the chymosin-sensitive region of bovine κ-casein (97−112), to both enzymes have previously been presented. Computational alanine scanning for mutating 39 residues in the substrate and the bovine enzyme are presented herein, and warm- ($\Delta\Delta G$ > 1 kcal/mol) and hot-spot ($\Delta\Delta G$ > 2 kcal/mol) residues in the bovine enzyme are identified. These residues are relevant for site-directed mutagenesis, with the aim of modifying the binding affinity and in turn affecting the catalytic efficacy of the enzyme.

KEYWORDS: *MM-PBSA, molecular dynamics, amber force field, binding, free energy calculations, mutation, milk, clotting, cheese, selectivity*

INTRODUCTION

Rennets are preparations of proteolytic enzymes that are used to initiate the first step of cheesemaking, the clotting of milk. Most preparations contain enzymes originally extracted from the stomachs of ruminant, mainly chymosin and pepsin, although proteases from plants or microorganisms are also in use today.[1] Chymosin is an aspartic protease found predominantly in the stomachs of mammalian infants, where its native function is to selectively cleave the milk protein κ-casein, causing the milk to curdle.[2] Chymosin, in contrast to other aspartic proteases (e.g., pepsin), exhibits a low general proteolytic activity,[3] a quality that makes it favored in cheese production. Bovine chymosin has been considered the most suitable enzyme for clotting of cow's milk due to its high specificity for cleaving the peptide bond between *Phe105*−*Met106* of bovine κ-casein (κ-casein residues are given in italics in the text throughout, whereas residues in chymosin are given in regular font). Recently, however, camel chymosin has proven to be superior to bovine chymosin in clotting cow's milk. Camel chymosin has a 70% higher clotting activity toward cow's milk compared to bovine chymosin. Furthermore, camel chymosin is more selective, reflected in a general proteolytic activity that is 5 times lower than that of bovine chymosin.[4] The two enzymes have high sequence identity (85%) and sequence similarity (94%),[5,6] which might help to explain why camel chymosin is able to clot cow's milk, but not why it does this so effectively. It is, conversely, then surprising that bovine chymosin is a very poor clotting agent toward camel's milk.[4] This disparity may be partially due to the lower sequence identity between camel and bovine κ-casein (69% for the 16 residues binding in the cleft on the enzyme);[6] however, a deeper understanding of the enzyme function holds industrial interest as both bovine and camel chymosin are sold as a clotting enzyme for cheese manufacturing.[1] Camel chymosin has recently been marketed as an alternative to bovine chymosin, offering higher yields and less bitter taste due to the lower nonselective proteolytic activity.[4,7]

X-ray crystal structures have been resolved of bovine chymosin in both apo-form (1CMS,[8] 3CMS,[9] 4CMS[10]) and cocrystallized with a bound norstatine-based inhibitor (1CZI).[11] Bovine chymosin is a globular protein consisting of 323 amino acid residues[2] that folds into a bilobal structure, with two similar β-barrel domains (Figure 1A). There is pseudosymmetry along a single cleft containing the catalytic residues Asp34 and Asp216 (chymosin numbering from PDB entry 1CMS[8]). A β-hairpin flap is found above the catalytic residues, making contacts with the substrate upon binding. The overall structure is common for cellular pepsin-like aspartic proteases, among which there is a high degree of structural homology.[12,13] The sequence identity between the N- and C-terminal domains of bovine chymosin is only 9%.[10] In contrast, the related, and more extensively investigated, viral retropepsin-like aspartic proteases, for instance, HIV proteases, are composed of two smaller identical β-barrel domains that together form a homodimer.[12] The catalytic residues, Asp34 and Asp216 in chymosin, both occur in an Asp-Thr-Gly sequence motif, which is conserved in the aspartic proteinase family of enzymes.[14] The side chains of the catalytic aspartic acid residues are oriented toward each other, in an approximate planar geometry with a water molecule positioned between the two catalytic residues in the three apo crystal structures of

Received: May 14, 2013
Revised: July 5, 2013
Accepted: July 8, 2013
Published: July 8, 2013

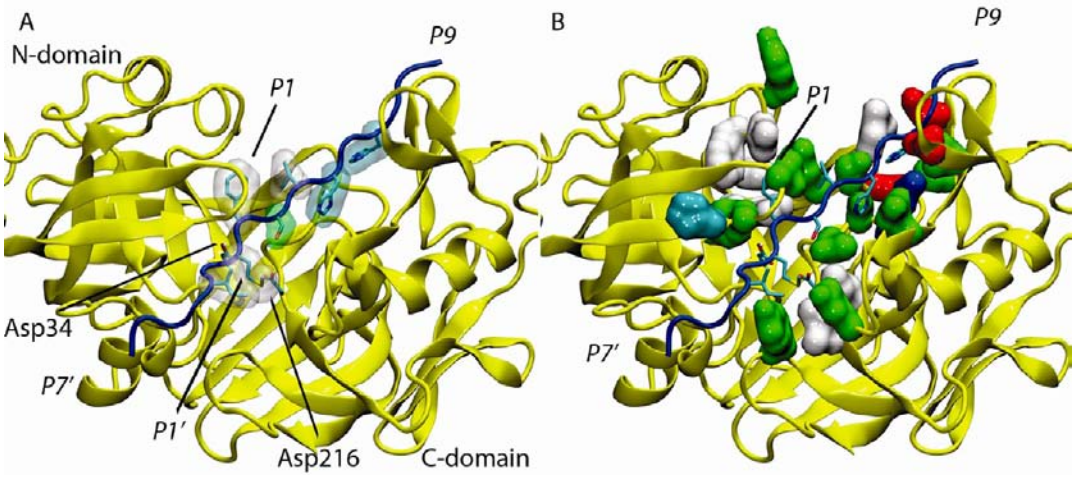

Figure 1. Molecular model of bovine chymosin shown in yellow, complexed with a fragment of bovine κ-casein, where the backbone is shown in blue and the side chains of interest are shown by cyan sticks. The two catalytic aspartic acids (Asp34 and Asp216) of chymosin and the bovine κ-casein *P1Phe* and *P1′Met* residues are included and colored by atom type (carbons in cyan). The residues for which alanine scanning calculations have been performed are indicated with a van der Waals surface. The colors of the surfaces are based on the residue type defined by VMD:[59] basic (blue), acidic (red), polar (green), and nonpolar (white). To highlight their position, the histidine residues have been colored cyan. In (A) the mutated residues of bovine κ-casein is shown with a transparent surface, and in (B) the residues that were mutated in bovine chymosin are marked with an opaque surface.

chymosin. A recent rerefinement of a crystal structure of the aspartic protease, apo plasmepsin II, has found that the two catalytic aspartic acid residues may not always be coplanar,[15] which has subsequently been supported by MD simulations of a few different aspartic proteases.[16] A network of hydrogen bonds called the fireman's grip stabilizes the catalytic aspartic acid residues[10,17,18] and also assists in holding the two domains together. The catalytic mechanism of hydrolysis is thought to involve a nucleophilic attack of a catalytic water molecule on the peptide carbonyl carbon, but the exact details of this mechanism are still being debated.[19,20] The reaction mechanism will not be discussed further in this paper, as the focus is on the free energies of binding for the substrate.

Four different types of casein, α_{s1}-, α_{s2}-, β-, and κ-casein, are found in milk.[21] The role of κ-casein, which consists of 169 residues,[22] is to help solubilize the three other caseins by promoting the formation of casein micelles.[21] In these molecular aggregates, κ-casein is predominantly found on the surface with its hydrophilic C-terminal pointing into the solvent.[23] Chymosin cleaves off the C-terminal part of κ-casein at the scissile bond (i.e., *Phe105−Met106*), which destabilizes the micelles and causes precipitation of the casein proteins. A sequence alignment of κ-casein from cow, camel, and other domesticated animals is shown in Figure 2 (only the residues that bind in the cleft of chymosin are shown). In this paper, the Schechter and Berger nomenclature will be used to refer to the peptide side chains and to the pockets of residues in the protein that interact with them.[24] For example, *Pn* and *Pn′* are used to denote κ-casein residues on either side of the scissile bond, where *n* increases with the distance from the scissile bond (Figure 2). Similarly, Sn and Sn′ denote the corresponding pockets in the enzyme that interact with the *Pn* and *Pn′* peptide side chains, respectively. Previous structural analysis using available X-ray crystal structures has determined the composition of amino acids making up seven of the pockets (S4 to S3′) in bovine chymosin.[8,10,11] It has furthermore been shown for bovine chymosin that the *P8−P7′* residues are located in the binding cleft during catalysis and that the *P9* residue, which is conserved in κ-casein, probably also binds to the enzyme.[25,26]

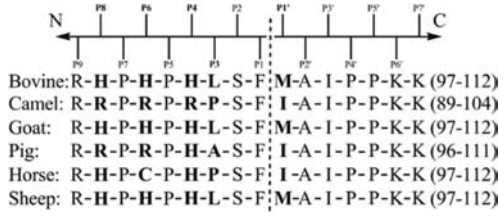

Figure 2. Aligned sequences of the chymosin-sensitive region of κ-casein in different domesticated animals. The *Pn* and *Pn′* numbering follows the Schechter and Berger nomenclature,[24] where *n* increases with the distance from the scissile bond (indicated by the dotted vertical line). The residues that differ between some of the species are highlighted in bold. The residue numbers are shown to the right in parentheses. The complete bovine κ-casein protein contains 169 residues.[22]

No X-ray or NMR structural data are currently available for bovine κ-casein. Therefore, in previous work,[25] we developed a model of bovine chymosin complexed with a 16 amino acid fragment of the chymosin-sensitive region of bovine κ-casein *P9−P7′*. The model was developed using molecular docking calculations, conformational search algorithms, and molecular dynamics simulations. The derived model is in good agreement with the limited experimental data about the complex, and it correctly predicts the existence of the fireman's grip hydrogen bonding network. A stable active site with geometries appropriate for nucleophilic attack on the peptide bond carbonyl carbon by the catalytic water molecule is found from MD simulations. Additionally, the residues of κ-casein were correctly positioned around the active site in accordance with X-ray crystallographic structures and kinetic data.[25] Subsequently, to describe the structural differences related to enzymatic action between bovine and camel chymosin toward bovine and camel κ-casein, we used this model as a template to develop homology models of the three remaining complexes (BOV/CAM, CAM/CAM, and CAM/BOV;[6] a slash-separated

nomenclature is used to distinguish the different chymosin/κ-casein complexes; e.g., CAM/BOV refers to the complex of camel chymosin with bovine κ-casein).

In this work, we have calculated the free energy of binding the substrate peptide (a fragment of bovine κ-casein) to both bovine and camel chymosin using the molecular mechanics Poisson−Boltzmann surface area (MM-PBSA) method.[27] Several methods are available for calculating the binding free energies of protein−ligand complexes at various degrees of accuracy.[28] Free energy perturbation (FEP)[29] and thermodynamic integration (TI) methods[30] are both thermodynamically rigorous and in principle very accurate,[28] but require a great deal of simulation time to provide adequate sampling, which makes them less suitable for a peptide substrate consisting of 16 amino acid residues. Many different end-point techniques have been developed to estimate binding free energies at lower computational expense, for example, the linear interaction energy (LIE) approach[31] and the MM-PBSA method. MM-PBSA is relatively fast and has been shown to afford reasonably accurate estimates of the binding free energy for similar systems.[27,32,33] In this paper, we present MM-PBSA alanine scanning calculations of 7 of the 16 amino acid residues in the κ-casein fragment in both the BOV/BOV and CAM/BOV complexes. Additionally, to investigate the chemical properties of the binding pockets in chymosin, we present alanine scanning calculations for 25 residues in bovine chymosin that interact with residues of the bovine κ-casein peptide fragment. These results assist in providing a quantitative description of the binding interactions between bovine chymosin and bovine κ-casein, highlighting hot-spot residues in the enzymes that are predicted to contribute significantly to the binding energy.

MATERIALS AND METHODS

Simulations. The chymosin−casein models and MD simulations used for calculating the binding free energies have previously been reported.[6,25] In short, after equilibration, in which the system was heated to 300 K in a multistep protocol, 96 ns of production MD was collected for each complex (BOV/BOV and CAM/BOV) in the NPT ensemble using the Amber03 force field and the TIP3P water model for explicit modeling of water molecules. For each of the calculations described below, 480 snapshots spread evenly from each of the 96 ns molecular dynamics trajectories of the complexes were used, resulting in time intervals of 200 ps between each snapshot. The explicit water molecules and ions were removed from the trajectory snapshots before energy calculations.

Free Energy Calculations. Free energy calculations were performed using the MM-PBSA method.[27,34] The main equations are shown here, where G denotes the Gibbs free energy:

$$\Delta G_{\text{binding}} = G_{\text{solvated}}(\text{complex}) - [G_{\text{solvated}}(\text{enzyme}) + G_{\text{solvated}}(\text{substrate})]$$

The free energies of each species were evaluated by the following relationships, where T is the temperature, S is the entropy, E is the potential energy, evaluated as the terms in molecular mechanics force field energy, used in place of the enthalpy,[27,32,34−36] and angled brackets denote an ensemble average:

$$G_{\text{solvated}} = \langle G_{\text{gas}} \rangle + \langle G_{\text{solvation}} \rangle - TS$$

$$\langle G_{\text{solvation}} \rangle = \langle E_{\text{PB}} \rangle + \langle E_{\text{cavity}} \rangle$$

$$\langle G_{\text{gas}} \rangle = \langle E_{\text{internal}} \rangle + \langle E_{\text{elec}} \rangle + \langle E_{\text{vdW}} \rangle$$

$$\langle E_{\text{internal}} \rangle = \langle E_{\text{bond}} \rangle + \langle E_{\text{angle}} \rangle + \langle E_{\text{torsion}} \rangle$$

The contributions to the solvation free energy are split into a nonpolar part (E_{cavity}) and a polar part (E_{PB}). For each calculation of solvation free energy (i.e., for enzyme, substrate, and complex), the nonpolar solvation term describes the process of transferring a nonpolar molecule in the shape of the molecule of interest from vacuum to water, including the creation of a cavity in water and the van der Waals interactions between the nonpolar molecule and the water molecules. The polar solvation term describes the contribution to the free energy due to polarization of the solvent environment by the solute.

The two polar terms, the Coulomb interaction energy (E_{elec}) and the polar contribution to the solvation free energy (E_{PB}), are both large numbers, compared to most other contributions, and the terms are often strongly anticorrelated; it therefore makes sense to calculate a combined term for the polar contribution to the binding (E_{polar}) that combines these two terms. Similarly, the nonpolar contributions to the binding (E_{vdW}) and (E_{cavity}) can be combined into one term (E_{nonpolar}), although these numbers are smaller in magnitude and are not necessarily correlated:

$$\langle E_{\text{polar}} \rangle = \langle E_{\text{elec}} \rangle + \langle E_{\text{PB}} \rangle$$

$$\langle E_{\text{nonpolar}} \rangle = \langle E_{\text{vdW}} \rangle + \langle E_{\text{cavity}} \rangle$$

The calculations were performed using the end-point method on single trajectories of each complex,[37] which is computationally less demanding than using separate trajectories for the enzyme, substrate, and complex. Furthermore, this approach has been shown to provide results that are close to experimental values due to cancellation of errors.[32,35] As described, all explicit water molecules were removed before these calculations, as required with the continuum solvent model. Although there are bridging water molecules, these do not influence the binding free energy results (data not shown). The calculations were performed with the MMPBSA.py module[38] of AMBER 11.[39] All nonbonded interactions were calculated without a cutoff. The dielectric constants of the solute and solvent were set to 1 and 80, respectively, which is default in MMPBSA.py and commonly done in MM-PBSA calculations. The default size of the solvent probe for the PB energy grid was set to 1.4 Å, and a default grid spacing of 0.5 Å was used. The ionic strength was set to 0.07 mol dm^{-3} to match the conditions in the simulation and to mimic the environment in milk. The entropic contributions to the binding free energy were calculated in the NAB module of AMBER 11, which derives translational, rotational, and vibrational entropies from molecular mass, principal moments of inertia, symmetry factor, and vibrational frequencies determined from normal-mode analysis. Before the normal mode calculations, each snapshot of the complex was minimized, as required for normal-mode analysis,[40] with a generalized Born solvent model, using default parameters in the MMPBSA.py module.

The errors shown in the graphs were calculated using bootstrap resampling with 10000 data samples, which was found to be a sufficiently large number of samples to allow the standard error to converge. The numbers are very similar to estimating the standard error by dividing the standard deviation by the square root of the number of data points. The error calculations were performed in Matlab.[41]

Alanine Scanning Calculations. Alanine scanning calculations describe the effect, in terms of the difference in the free energy of binding, of mutating a specific amino acid side chain to a methyl group. Computational alanine scanning experiments were performed using the protocol of Massova and Kollman,[42] although we are subtracting the wild-type binding free energy from that of the mutant. Negative numbers thus indicate that a mutation to alanine results in an increased overall binding free energy, whereas positive numbers signify a reduced binding free energy, contrary to the scheme by Massova and Kollman.

$$\Delta\Delta G_{\text{binding}} = \Delta G_{\text{binding\_mutant}} - \Delta G_{\text{binding\_wildtype}}$$

The unsigned error of calculations of this nature has previously been reported to be 1 kcal/mol.[42,43] The results highlight so-called warm-

(>1 kcal/mol) or hot-spot (>2 kcal/mol) residues that contribute disproportionately to the binding free energy.[42−44] Owing to the prohibitive computational cost, and in accordance with previous studies,[42,43,45] the entropy term was neglected. Additionally, we calculate two new terms to determine the electronic nature of the energy lost or gained as a result of alanine scanning.[42,43] This partitioning is similar to the terms above for the overall binding free energy. First, a polar term is computed that takes into account the Coulomb interaction energy (E_{elec}) and the polar contribution to the solvation free energy (E_{PB}), because it has been shown that a change in one term is in most cases strongly anticorrelated with a change in the other term ("variant" in the equation signifies either the wild type or the mutant),[42,43]

$$\Delta\Delta E_{polar} = \Delta E_{polar\_mutant} - \Delta E_{polar\_wildtype}$$

$$\Delta E_{polar\_\{variant\}} = \Delta E_{elec\_\{variant\}} + \Delta E_{PB\_\{variant\}}$$

Second, a nonpolar term is defined that takes into account the van der Waals interaction energies (E_{vdW}) and the nonpolar contribution to the solvation free energy (E_{cavity}).

$$\Delta E_{nonpolar} = \Delta E_{nonpolar\_mutant} - \Delta E_{nonpolar\_wildtype}$$

$$\Delta E_{nonpolar\_\{variant\}} = \Delta E_{vdW\_\{variant\}} + \Delta E_{cavity\_\{variant\}}$$

The partitioning of $\Delta\Delta G$ into the two terms allows for a deeper understanding of the underlying interactions and extends the alanine scanning calculation method to highlight residues that would traditionally not be classified as hot-spot residues solely on the basis of $\Delta\Delta G_{binding}$, yet display a potential for modification based on either $\Delta\Delta E_{polar}$ or $\Delta\Delta E_{nonpolar}$. This method uses the same trajectories as for the MM-PBSA calculations and is calculated using MMPBSA.py[38] in AMBER 11. Individual terms ($\Delta\Delta E_{PB}$, $\Delta\Delta E_{elec}$, $\Delta\Delta E_{cavity}$, and $\Delta\Delta E_{vdW}$) have been calculated as standard by MMPBSA.py. The two additional terms have been calculated using an in-house Matlab script. For each alanine scanning mutation, the side-chain atoms of the selected amino acid residue were removed, so that only the backbone and the C_β atom with up to two hydrogen atoms remained; the remaining hydrogen atoms were subsequently added.

The mutation to alanine is introduced after the simulation has been performed, and it is thereby assumed that the structural perturbations of the system upon such a mutation are small and will not have a major effect on the dynamics of the enzyme−substrate complex, implying that the binding free energy may be obtained from a single trajectory of the complex of the wild-type system. The single trajectory approach is computationally much less demanding than performing MD simulations for each mutant, which is an important consideration given the number of residues being mutated in this study. A recent study by Bradshaw et al. supports the validity of this argument.[45] Furthermore, use of the same trajectories allows for cancellation of errors, which has proven to give more accurate results.[42,43]

To be conservative, alanine scanning calculations have been performed only for residues where the root-mean square fluctuation (RMSF) is near or below 2 Å (see Figure S1 in the Supporting Information), where the binding interaction can be said to be reasonably well described. Using this criterion, we have excluded the two residues in each termini of the substrate (*P9*−*P8* and *P6′*−*P7′*), as well as the *P2′* residue because this is already an alanine. Furthermore, in accordance with earlier studies, we have excluded the proline residues (*P7*, *P5*, *P4′*, *P5′*) because the backbone conformation of proline differs significantly from that of alanine.[42,46] In total, alanine scanning calculations were performed for 7 of the 16 residues of the κ-casein fragment in both the BOV/BOV complex and the CAM/BOV complex (Figure 1A). Moreover, alanine scanning calculations were performed on chymosin in the BOV/BOV complex for residues having side chains that interact with a side chain of any of the 7 residues in the κ-casein fragment based on a condition of spatial proximity and frequency; that is, heteroatoms <4 Å apart in >5% of the snapshots collected from the MD simulation (Figure 1B). The full list of residues scanned in bovine chymosin can be found in the Supporting Information (Table S3). Alanine scanning was naturally not performed on the two catalytic aspartic acids (Asp34 and Asp216).

Degree of Burial Calculations. Alanine scanning calculations have a tendency to overestimate the energy of buried residues involved in salt bridges.[43] Therefore, we have calculated the degree of burial of each residue in the κ-casein fragment that we have mutated, using the following relationship, where the area is the solvent accessible surface area (SASA), calculated in VMD with a probe sphere of 1.4 Å,[43] and where SASA_complex and SASA_unbound are the solvent-accessible surface areas of the given residue in the complex and in the unbound peptide, respectively (the numbers are reported in the Supporting Information, Tables S1−S3).

$$\text{degree of burial (\%)} = 100(1 - \langle \text{SASA\_complex} \rangle / \langle \text{SASA\_unbound} \rangle)$$

RESULTS AND DISCUSSION

Binding Free Energy Calculations of Wild-Type Complexes. The binding free energies of the two complexes were calculated using the MM-PBSA methodology.[27,34] The numbers are subdivided into the different terms of the free energy as shown in Table 1. The results show that binding the

Table 1. Different Components of the Binding Free Energy of the Two Complexes Calculated from Their Trajectories[a]

	BOV/BOV		CAM/BOV	
contribution	mean	SE	mean	SE
ΔE_{vdW}	−143.5	0.5	−139.4	0.5
ΔE_{elec}	−1245.4	3.9	−888.4	2.7
ΔE_{PB}	1308.0	3.7	960.2	2.5
ΔE_{cavity}	−15.3	0.0	−14.8	0.0
ΔE_{polar}	62.6	0.5	71.8	0.6
$\Delta E_{nonpolar}$	−158.9	0.5	−154.2	0.5
ΔG_{gas}	−1389.0	4.1	−1027.8	2.8
ΔG_{solv}	1292.7	3.7	945.3	2.5
$\Delta G_{subtotal}$	−96.3	0.7	−82.5	0.6
$T\Delta S$	−53.5	0.5	−49.0	0.5
ΔG	**-42.8**	0.7	**-33.4**	0.8

[a]BOV/BOV and CAM/BOV are, respectively, the bovine and the camel chymosin enzymes complexed with a fragment of bovine κ-casein. The data presented in this table are ensemble averages, and standard errors of the mean (SE) were determined by bootstrap resampling. All values are in kcal/mol.

κ-casein fragment in chymosin is favorable in both complexes (Table 1). The entropic contributions to the binding free energy are comparable, which was expected given the similar structures and levels of dynamics in the systems, although the BOV/BOV system has a slightly higher entropy contribution.[6] The largest differences in the binding are a result of changes in both the electrostatic energy (ΔE_{elec}) and the polar solvation contribution (ΔE_{PB}) to the binding energy. These two terms are anticorrelated, and summing them results in the polar contribution to binding (ΔE_{polar}), which is unfavorable in both enzyme−substrate complexes. Thus, it is the nonpolar contributions to the binding free energy that make the complexation favorable, which suggests that the electrostatics serve a different role. For example, they may facilitate substrate

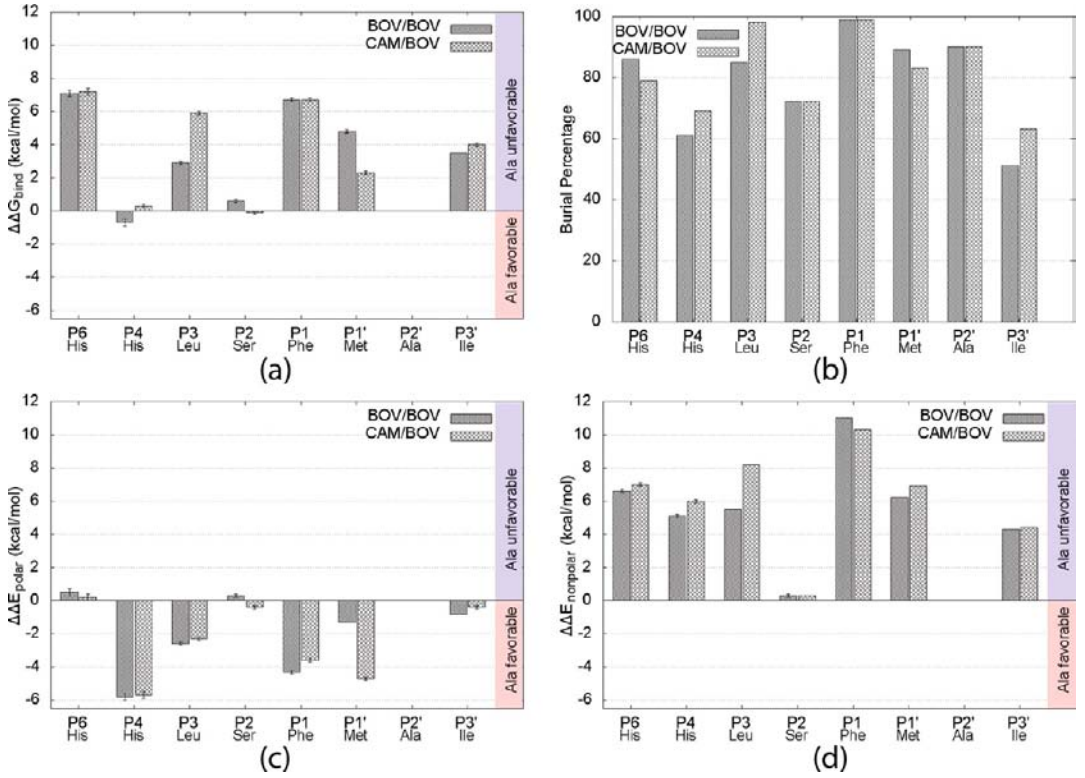

Figure 3. Comparison of the seven residues probed in bovine κ-casein in the two enzymes bovine and camel chymosin in terms of (a) the $\Delta\Delta G$ of binding from the alanine scanning calculations, (b) the degree of burial each residue experiences upon binding, (c) the $\Delta\Delta E_{polar}$ from the alanine scanning calculations, and (d) the $\Delta\Delta E_{nonpolar}$ from those same calculations. In all instances, positive values indicate the alanine substitution is unfavorable, whereas negative values indicate a favorable substitution, as indicated by the blue and red sidebars.

recognition,[47] determine specificity, and drive product dissociation following substrate cleavage. The binding affinity of the bovine κ-casein fragment to camel chymosin (−33.4 kcal/mol) is less favorable than binding to bovine chymosin (−42.8 kcal/mol). This difference arises from a few factors; both the polar and nonpolar contributions to the binding free energy are more favorable, by −9.2 and −4.7 kcal/mol, for the BOV/BOV complex and are only counteracted by a −4.5 kcal/mol higher loss of entropy, likely due to this stronger binding. The stronger binding is correlated with a lower RMSF for most of the κ-casein residues in the BOV/BOV complex, compared to the CAM/BOV complex (see Figure S1 in the Supporting Information).

It is important to note that these numbers address only the strength of the interaction between the enzyme and substrate when complexed; neither initial recognition and association nor dissociation are adequately described as both of these processes may involve conformational change. Moreover, these numbers are difficult to compare to experiments as most experiments report kinetics data, specifically, the Michaelis−Menten constant (K_M) and the turnover number (k_{cat}), and whereas K_M is at times referred to as a binding affinity, the K_M values cannot be directly compared to free energies of binding. Further difficulties originate in experimental conditions (pH, temperature, ionic strength, concentrations, and purity) and use of substrates, as either small peptides, κ-casein in solution, or whole casein micelles. Reported K_M values vary by several orders of magnitude (7.59×10^{-4}, 0.165, or 0.21 mM, respectively),[4,48,49] due to, in part at least, different reaction conditions. The trends between the experimental K_M values of different enzymes and substrates do not provide a conclusive picture about which enzymes are best at cleaving bovine κ-casein,[4,48,49] although it is known that camel chymosin is superior at clotting cow's milk on the basis of yield and characteristics such as the industrial term C/P, which is a relationship between the clotting time (C) and cleavage specificity (P).[4]

Alanine Scanning Calculations on Bovine κ-Casein in the Two Chymosin Enzymes. To evaluate the origin of the difference in the binding free energy, alanine scanning calculations have been performed for 7 of the residues of the κ-casein fragment in both the BOV/BOV and the CAM/BOV complex from 96 ns MD simulations of each complex. The results allow us to approximately quantify the effect that differences in the primary structure of bovine and camel chymosin have on the energetics of bovine κ-casein binding, focusing on the interaction with the functional groups of the side chains of the amino acids. The binding is, as shown above, stronger in the BOV/BOV complex compared to the CAM/BOV complex by 9.4 kcal/mol (Table 1). The differences in the alanine scanning results for the 7 residues in κ-casein are shown in Figure 3a (the values for the individual terms are reported in the Supporting Information; Table S1 for residues in the substrate for the BOV/BOV complex and Table S2 for residues in the substrate for the CAM/BOV complex). The result of an alanine scanning calculation is the $\Delta\Delta G$ that describes the predicted consequences of mutating the side chain to a methyl group. A negative $\Delta\Delta G$ here indicates that the binding free energy will be stronger as a result of the mutation, whereas a positive number signifies a weaker binding. The burial of each residue is presented in Figure 3b, as it is known that salt bridges are overestimated with this method if a residue is significantly

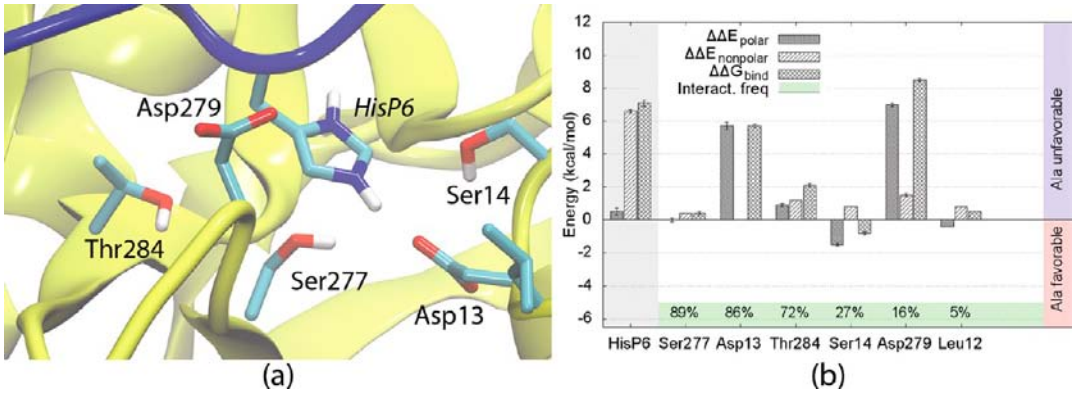

Figure 4. (a) Snapshot of *HisP6* residue after 90.6 ns of MD interacting with Asp13, which is a dominating interaction, as can be seen in (b), where the energy contributions to the binding, as computed by the alanine scanning method, are indicated for *HisP6* and residues in bovine chymosin that it interacts with. Error bars are the standard error calculated using bootstrap resampling. Light gray shading highlights the κ-casein residue, whereas chymosin residues are displayed in white background. The percentages indicate interaction frequency between this residue and κ-casein. The sidebars have identical meaning to those in Figure 3.

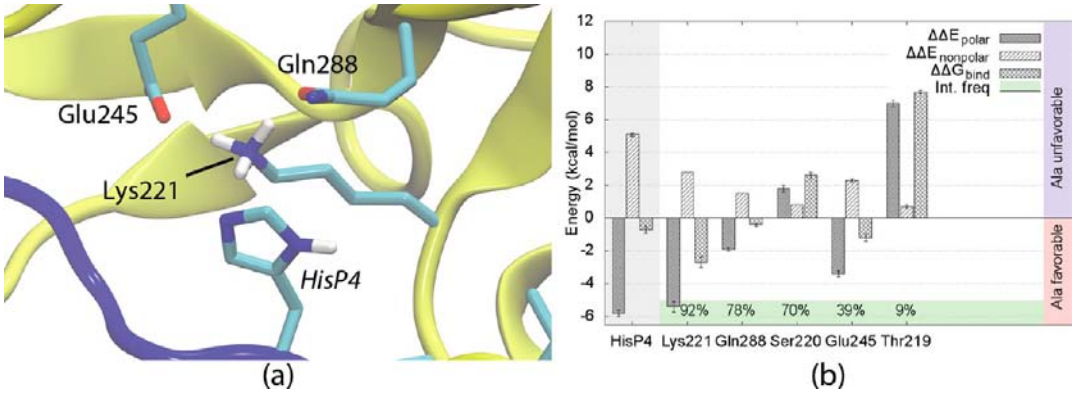

Figure 5. (a) Snapshot of *HisP4* residue at 57.4 ns interacting with Lys221, which in turn interacts with Glu245 via a salt bridge and Gln288 via a hydrogen bond. (b) Results of alanine scanning for *HisP4* and residues in chymosin that it interacts with. The percentages indicate interaction frequency between this residue and κ-casein. Gray shading highlights the κ-casein residue. Same coding as in Figure 4.

buried. The $\Delta\Delta G$ can be separated into two terms, $\Delta\Delta E_{polar}$ and $\Delta\Delta E_{nonpolar}$, shown in panels c and d, respectively, of Figure 3.

The change in free energy of binding for each of the seven residues in the substrate when bound in either of the two enzymes are very similar, reflecting a similar binding and local environment surrounding the residue. Interesting differences are found for residues *HisP4*, *LeuP3*, *SerP2*, and *MetP1′*, which bind in pockets that are chemically different in bovine and camel chymosin. Although it is the enzyme, and not the substrate, that is the target of protein engineering, it is interesting to predict what alterations in the substrate could lead to a different binding affinity. Of the seven point mutations to κ-casein that were tested during the alanine scanning calculations, only the *HisP4Ala* mutation in the BOV/BOV complex was found to be favorable. That none of the other residues are very favorable to mutate to alanine is largely due to the fact that the nonpolar interactions contribute significantly to the binding energy; the magnitude seems to be correlated with the size of the residue being mutated to alanine. Contrastingly, when polar contributions are considered (Figure 3c), it is favorable to mutate most residues to alanine, particularly for *HisP4*, *LeuP3*, *PheP1*, and *Met P1′*; on the basis of polar interactions alone, these four residues could be classified as warm- or hot-spot residues. This suggests that mutations that remove unfavorable polar interactions, while retaining nonpolar interactions, would be expected to increase the binding free energy, for example, changing a polar residue to an equally sized nonpolar residue. It is not of relevance for protein engineering to mutate the substrate for cheese production. It is, however, more relevant to predict mutations in chymosin, because this has been cloned, making engineered mutants possible to produce.

Alanine Scanning Calculations of the Bovine Chymosin and Bovine κ-Casein Complex. Bovine chymosin has been sold commercially since 1874, whereas the camel variant of the enzyme was introduced to the market only recently, and therefore most of the biochemical data available on substrate binding to chymosin is for the bovine variant. Each binding pocket in the bovine enzyme has previously been experimentally probed using a variety of binding fragments to describe the local chemical properties.[18] Bovine and camel chymosins have both been cloned, making it possible to engineer this enzyme. In the following, the results will be presented in detail for the individual specificity pockets matching the seven substrate residues probed above for the BOV/BOV complex (the values for the individual terms are reported in the Supporting Information, Table S3). To ease comparison, the *Pn* residue will be presented alongside the pocket residues in the following.

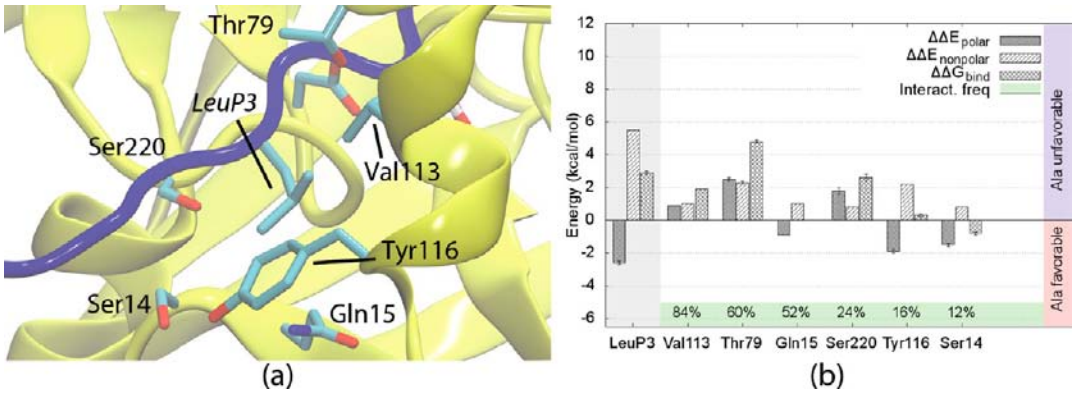

Figure 6. (a) Snapshot of the *LeuP3* residue at 41.8 ns and (b) results of alanine scanning for *LeuP3* and residues in chymosin that it interacts with. Gray shading highlights the κ-casein residue. Same coding as in Figure 5.

Although significant, the binding contribution from *HisP6* upon mutation to an Ala residue in the S6 pocket is almost purely nonpolar, despite being modeled with a formal charge of +1 (Figure 4). This observation is based on the fact that the penalty of removing the electrostatic interaction ($\Delta\Delta E_{elec}$ = 303.4 kcal/mol) almost completely cancels out the change in the polar solvation free energy ($\Delta\Delta E_{PB}$ = −303.0 kcal/mol, see Table S3). The S6 residues are mainly polar, and this pocket can favorably be filled with water when a substrate is not present. When bound, the *HisP6* and Asp13 interact 86% of the time, primarily by a salt bridge. The effect of mutating Asp13 to alanine eliminates the salt bridge, resulting in a significant loss of polar binding energy (∼6 kcal/mol), which may suggest that Asp13 helps stabilize the charged histidinium form of *HisP6*. MM-PBSA alanine scanning calculations are known to overestimate buried salt-bridge interactions,[42,43] and *HisP6* is 86% buried in the complex (see Figure 3b), yet even at a smaller magnitude this is expected to be a crucial interaction. The Ser14 residue is the only residue in the pocket that is favorable to mutate to alanine, primarily because the polar part of Ser14 is not favorable for the binding. The nonpolar part of the residue does contribute to the binding, and instead of mutating this residue to alanine, a small hydrophobic residue might improve the binding within this pocket.

As shown in Figures 3 and 5, the *HisP4Ala* mutation is the only side chain of the seven residues that is predicted to increase the binding affinity. However, although removing the polar interactions is highly favorable, the loss of nonpolar contributions is nearly as unfavorable, and the mutation contributes only slightly to the binding free energy. This suggests that a large nonpolar residue will be highly favorable in this position and correlates with earlier studies showing that a charged lysine residue is particularly unfavorable in this position.[50] There are significant unfavorable polar interactions in the S4 pocket when binding a polar residue (Figure 5). For example, mutations of either Lys221, Glu245, or Gln288 to alanine are all favorable. Thus, removing the polar interactions improves the binding free energy. On the basis of the computed free energy changes for Ala mutations, Lys221 and Glu245 are classified as hot- and warm-spots, respectively. Furthermore, whereas the contribution to the binding free energy of each individual residue is relatively small, collectively, the results may suggest that alterations of this pocket could be favorable with the objective of increasing the binding affinity, by, for example, mutation of one or more residues. Most importantly, the results indicate that replacing the positively charged hot-spot residue, Lys221, with a similar sized hydrophobic residue should be favorable, as the favorable nonpolar interactions will be retained. The same trend can be observed for Glu245 and Gln288. Interestingly, in camel chymosin residue 221 is indeed a valine.[6,25] Assuming that *HisP4* in κ-casein predominantly binds with a neutral side chain, the S4 pocket could be tailored to better accommodate the *HisP4* residue. The charged Lys221, which we found to be a hot-spot residue, should in this case be mutated to a less polar residue, for example, Met, Leu, Ala, Ile, or Val (as in camel chymosin), to retain the important nonpolar interactions and remove the unfavorable polar interactions. Alterations could also be made to Glu245, which we found to be a warm-spot residue. Correspondingly, altering Glu245 to a neutral residue, for example, Gln, Leu, Ala, Met, or Ile, is expected to improve the binding free energy, as the nonpolar interactions have proven important for this residue also. Similarly, Gln288 could also be modified to a less polar residue of rougly the same size. On the other hand, if *HisP4* binds in its charged (histidinium) form, then mutation of Lys221 like in camel chymosin (Val221) is still recommended, but then the pocket could be tailored to stabilize the positive charge with Gln288Glu without changing Glu245. The pH of milk is close to the pK_a of histidine and, therefore, histidine may exist in multiple tautomer forms and charge states, which could be worth exploring further, particularly as pH is known to modulate enzyme activity.[18] In general, aspartic proteases favor hydrolysis at acidic pH, but in the case of chymosin it has adapted to a neutral pH environment at the start of cheesemaking. In the latter stages of cheesemaking the pH drops, but most of the κ-casein has been cleaved at this point.

The S8−S4 pockets have previously been shown to be important for binding. It has been demonstrated that the rate of hydrolysis is ∼18-fold higher for the fragment *P8*−*P4*′ compared to the *P3*-*P4*′ fragment.[3,51] Experimentally, it is known that the dipeptide H-Phe-Met-OH is not easily hydrolyzed by bovine chymosin and neither are tri- or tetrapeptides containing the scissile bond.[52] Hill stated, on the basis of a series of experiments, that other residues were needed to modulate the binding and subsequent cleavage. In particular, residues *HisP6* and *HisP4* were implicated as important modulators of this effect,[53] a conclusion consistent with our modeling efforts and the strong interactions between *HisP6* and Asp13 that we have observed. Additionally, there is a persistent interaction between Asp13 and *HisP8*.[6,25]

The side chain of the *LeuP3* is also important for binding of κ-casein. Surprisingly, the relatively small side chain contributes

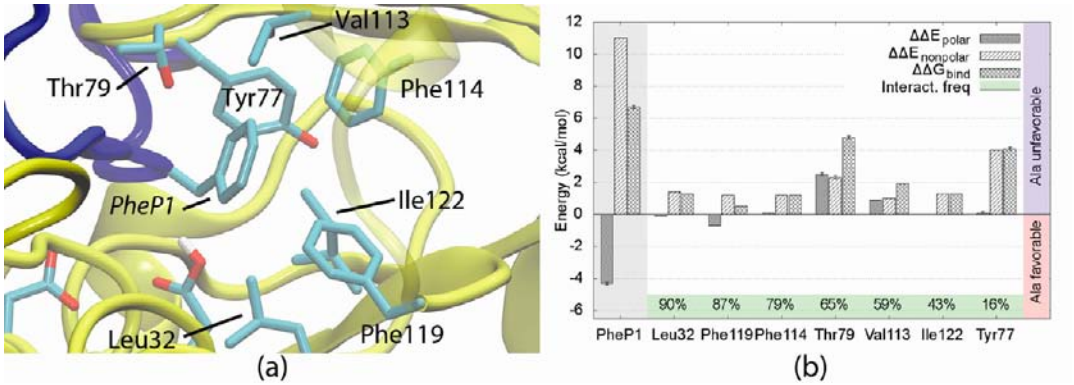

Figure 7. (a) Snapshot of *PheP1* residue at 41.8 ns enclosed in the S1 pocket and (b) results of alanine scanning for *PheP1* and residues in chymosin that it interacts with. Gray highlights the κ-casein residue. Same coding as in Figure 5.

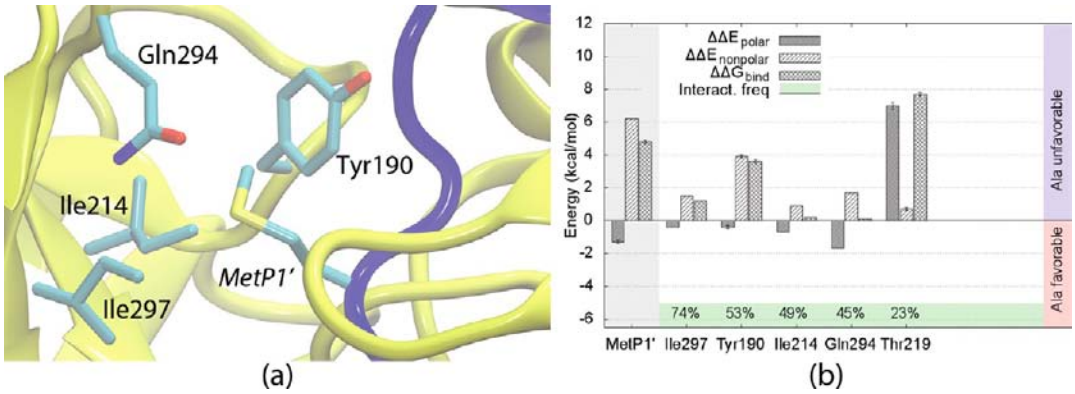

Figure 8. (a) Snapshot of *MetP1′* residue at 41.8 ns near Ile297 and the aromatic ring of Tyr190 and (b) results of alanine scanning for *MetP1′* and residues in chymosin that it interacts with. Gray shading highlights the κ-casein residue. Same coding as in Figure 5.

significant nonpolar interaction energy to the binding. Mutating this residue to an alanine is favorable only in terms of polar interactions due to favorable changes in the solvation term, but overall the unfavorable nonpolar terms dominate, and this mutation results in a weaker binding free energy (Figure 6). It has been shown that isoleucine and valine are favored at *P3* in the substrate,[18] which reflects the similarity in terms of size and chemistry to leucine. The result here is consistent with mutagenesis studies showing that catalysis is promoted by aliphatic residues, tolerated by hydrophilic residues, and disfavored by proline and positively charge residues at this position.[54,55] These observations are interesting as the *P3* position in camel κ-casein is a proline residue, which may indicate why bovine chymosin only poorly clots camel's milk.[4] Furthermore, according to observations by Hill, the protease activity is not present unless a residue occupies the *P3* position.[52,53] The S3 pocket is small as shown in Figure 6a. The nonpolar interactions that *LeuP3* forms are mainly with Val113 and Thr79, the latter of which points its nonpolar methyl group toward *LeuP3*. In the S3 pocket, the residues in bovine and camel chymosin are identical, but they are slightly differently organized, due to changes in the neighboring S1 pocket, Leu32 and Val32, respectively. This conformational rearrangement, which increases the interaction between the *LeuP3* residue and Phe119, might be one possible explanation for the observed difference (3 kcal/mol) in the alanine scanning results for the *P3* residue in the BOV/BOV and CAM/BOV complexes (Figure 3). Our results suggest that a mutation in the S1 pocket (Leu32Val, as it is in camel chymosin) could improve the binding of the *LeuP3* residue.

The *SerP2* residue side chain contributes little to the binding, and the removal of the OH group makes only minor changes to the nonpolar term (see the Supporting Information, Figure S2). The S2 pocket has been shown to be of low specificity, and it can accommodate tyrosine, valine, and serine in the substrates.[18] Whereas the contribution to the binding free energy is minor, it has been suggested that the chemical characteristics of the *SerP2* position are crucial for enzyme action in bovine chymosin.[52] Our previous studies indicated that a hydrogen bond chain is formed from the *SerP2(OH)* to Thr219(OH) and onward to Asp216(Oδ), assisting in keeping the two carboxyl groups of the catalytic aspartates coplanar.[6,25] The interactions formed by Thr219 are very favorable to the binding free energy, particularly in terms of the polar contribution to the energy (Figure S2b). Bovine and camel chymosin differ by a Val to Phe change at position 223 in the S2 pocket, which contributes to the small difference in ΔΔ*G* observed for the alanine scanning results for the *P2* residue in the BOV/BOV and CAM/BOV complexes (Figure 3).

The alanine scanning results also clearly reveal the importance of the hydrophobic nature[18] of the S1 pocket (Figure 7). For example, mutating the *PheP1* residue to an alaine residue is highly unfavorable due to loss of the significant nonpolar interactions (∼11 kcal/mol). Similarly, the residues forming the S1 pocket are mostly hydrophobic, and all contribute evenly to the nonpolar binding free energy terms. Experiments have shown that if *PheP1* is replaced by the bulkier

Phe(NO_2) or cyclohexylamine analogues, the substrates are still hydrolyzed, albeit at a lower rate.[56]

The results show that the *MetP1′* side chain is also important for binding, again mostly due to nonpolar interactions (Figure 8). Bovine chymosin has been shown to cleave human and porcine κ-casein (both being *PheP1*−*IleP1′*), and rat and mouse κ-casein (*PheP1*−*LeuP1′*),[56] indicating that the pocket is not specific for methionine, but does prefer less polar residues. A *MetP1*−*PheP1′* variant of bovine κ-casein is hydrolyzed 1.8 times more rapidly than the wild-type protein by bovine chymosin,[56] showing that neither of the *P1* and *P1′* pockets are highly selective, although both prefer hydrophobic residues. The methyl sulfide group on methionine interacts with the Gln294 residue, and removing this interaction is not favorable in electrostatic terms ($\Delta\Delta E_{elec}$ = 0.3 kcal/mol), but is favorable when polar solvation terms are considered ($\Delta\Delta E_{PB}$ = −1.9 kcal/mol, see Table S3 of the Supporting Information). The nonpolar contribution to the free energy comes from interactions with Ile297, Tyr190, and Ile214. It is further interesting in this context that position 294 in camel chymosin is a glutamate, as we have previously shown that *MetP1′* does not interact with Glu294 in the CAM/BOV complex,[6] which moves away from the S1′ pocket. Thus, this residue might be a good target for mutation. The alanine scanning results for the Gln294 residue indicate that the mutation does not affect binding free energy (Figure 8).

The results of alanine scanning on *IleP3′* show that it contributes to the binding mostly due to nonpolar interactions (see the Supporting Information, Figure S3), reflecting the hydrophobic chemical nature of this residue. The side chain of *IleP3′* makes consistent nonspecific interactions with Gln294, Tyr190, and His76, signified by interactions present <50% of the time. It is perhaps suprising that this highly conserved residue (see Figure 2) does not have a more defined binding motif. It is worth noting that Gln294 is contained in a highly flexible loop that was not solved in the crystal structure,[10] which might explain the intermittent frequency of this interaction. Furthermore, the two proline residues following it (*ProP4′* and *Pro5′*) restrict its mobility significantly, perhaps making it unable to form more favorable interactions.

In accordance with earlier studies, we have excluded the proline residues (*P7*, *P5*, *P4′*, *P5′*), because the backbone conformation of proline differs significantly from that of alanine. The key role of the proline residues is likely to be in correctly aligning the κ-casein residues in the pockets of chymosin, as has previously been suggested,[26,51] and to expose the peptide on the surface of the whole κ-casein molecule.[47]

In summary, in this study we have investigated the binding of bovine κ-casein to bovine and camel chymosin, with the aim of understanding the differences in binding that can help explain the catalytic efficacies observed during the initial stage of cheese production; the clotting activity of camel chymosin toward cow's milk is higher than that of bovine chymosin, and the cleavage is more specific toward the scissile *PheP1*−*MetP1′* bond.[4] We have calculated the Gibbs free energy of binding of a bovine κ-casein fragment in chymosin for both the native bovine and camel chymosins. Furthermore, we have investigated the influence of point mutations on the binding free energy by way of computational alanine scanning calculations. These results have allowed us to quantify the importance of specific polar and nonpolar interactions and to identify several warm- and hot-spot residues that contribute disproportionately to the binding free energy. It is worth remembering that although some residues do not contribute much to the binding free energy, these residues can have very specific interactions that assist in the correct binding of κ-casein to chymosin (e.g., Asp13 and *HisP8*) or the correct orientation of the catalytic aspartic acid residues (e.g., Thr219 and *SerP2*). We have made several suggestions for single point mutations with the aim of engineering an enzyme that will have a higher free energy of binding of the substrate. The mutations are focused in the S6, S4, S3, and S1′ pockets.

It is important to note that the binding free energy is only part of the enzymatic process, which also depends on other factors such as association/dissociation kinetics and covalent bond breaking and forming. Experimentally, only milk clotting rates, K_M, and k_{cat} have been measured for chymosin complexes,[4,48,49] which cannot be directly compared to binding free energies without making undue assumptions. Nevertheless, on the basis of the analysis presented here, several mutations can be identified that should improve the binding in the bovine chymosin−bovine κ-casein complex. The mutations we propose are primarily not to alanine, but are instead to residues selected on the basis of our analysis of the computed effect of an Ala mutation in terms of polar and nonpolar interaction energy responses.

Our conclusions are drawn on the basis of individual point mutations and, therefore, we caution that making all of the suggested mutations on one enzyme will perhaps not result in the expected change in enzymatic behavior, as there may be synergistic effects that we have not considered. Other factors in the catalytic activity of bovine chymosin, such as the self-inhibiting mechanism,[57] recognition, the encounter complex, and a pH switch observed in homologous proteins[58] are worth investigating. Studies are underway in our group to understand these, as are experimental efforts to evaluate the binding properties of some of the herein predicted mutants for improved binding of κ-casein to chymosin.

■ ASSOCIATED CONTENT

Supporting Information

Per residue RMSF of the bovine κ-casein fragment in both the bovine and camel enzyme complexes; results for the S2 and S3′ pockets; values of the alanine scanning terms for all reported calculations. This material is available free of charge via the Internet at http://pubs.acs.org.

■ AUTHOR INFORMATION

Corresponding Author

*(B.S.) Phone: +45 87 15 59 75. Fax: +45 86 19 61 99. E-mail: birgit@chem.au.dk.

Present Addresses

§(J.S.) Department of Chemistry and Biochemistry, University of California, San Diego, 9500 Gilman Drive, La Jolla, CA 92093, USA.

#(D.S.P.) Department of Physics, University of Strathclyde, 107 Rotten row, Glasgow G4 0NG, UK.

Funding

This work was supported by grants from the Villum Kahn Rasmussen Foundation, the BioSys Network, the Danish Council for Independent Research, the Danish National Research Foundation (DNRF59), and the Centre for Theory in Natural Sciences, Aarhus University. Computations were made possible through grants from the Lundbeck Foundation, the Novo Nordisk Foundation, the Carlsberg Foundation, and

the Danish Center for Scientific Computing. J.S. thanks the Alfred Benzon Foundation for a postdoctoral fellowship. D.S.P. is grateful for funding from the European Commission, through a Marie Curie Intra-European Fellowship within the seventh European Community Framework Program (No. FP7-PEOPLE-2010-IEF).

Notes

The authors declare no competing financial interest.

■ ACKNOWLEDGMENTS

We thank Drs. Karsten Bruun Qvist and Hans van den Brink from Chr. Hansen A/S for fruitful discussions.

■ REFERENCES

(1) Harboe, M.; Broe, M. L.; Qvist, K. B. The production, action and application of rennets and coagulants. In *Technology of Cheesemaking*, 2nd ed.; Law, B. A., Tamime, A. Y., Eds.; Wiley-Blackwell: Oxford, UK, 2010; pp 98−129.

(2) Foltmann, B.; Pedersen, V. B.; Kauffman, D.; Wybrandt, G. The primary structure of calf chymosin. *J. Biol. Chem.* **1979**, *254*, 8447−8456.

(3) Gustchina, E.; Rumsh, L.; Ginodman, L.; Majer, P.; Andreeva, N. Post X-ray crystallographic studies of chymosin: the existence of two structural forms and the regulation of activity by the interaction with the histidine-proline cluster of κ-casein. *FEBS Lett.* **1996**, *379*, 60−62.

(4) Kappeler, S. R.; van den Brink, H. J.; Rahbek-Nielsen, H.; Farah, Z.; Puhan, Z.; Hansen, E. B.; Johansen, E. Characterization of recombinant camel chymosin reveals superior properties for the coagulation of bovine and camel milk. *Biochem. Biophys. Res. Commun.* **2006**, *342*, 647−654.

(5) Larkin, M. A.; Blackshields, G.; Brown, N. P.; Chenna, R.; McGettigan, P. A.; McWilliam, H.; Valentin, F.; Wallace, I. M.; Wilm, A.; Lopez, R.; Thompson, J. D.; Gibson, T. J.; Higgins, D. G. ClustalW and ClustalX version 2. *Bioinformatics* **2007**, *23*, 2947−2948.

(6) Sørensen, J.; Palmer, D. S.; Qvist, K. B.; Schiøtt, B. Initial stage of cheese production: a molecular modeling study of bovine and camel chymosin complexed with peptides from the chymosin-sensitive region of κ-casein. *J. Agric. Food Chem.* **2011**, *59*, 5636−5647.

(7) Bansal, N.; Fox, P. F.; McSweeney, P. L. Factors that affect the aggregation of rennet-altered casein micelles at low temperatures. *Int. J. Dairy Technol.* **2008**, *61*, 56−61.

(8) Gilliland, G. L.; Winborne, E. L.; Nachman, J.; Wlodawer, A. The three-dimensional structure of recombinant bovine chymosin at 2.3 Å resolution. *Proteins* **1990**, *8*, 82−101.

(9) Strop, P.; Sedlacek, J.; Stys, J.; Kaderabkova, Z.; Blaha, I.; Pavlickova, L.; Pohl, J.; Fabry, M.; Kostka, V. Engineering enzyme subsite specificity: preparation, kinetic characterization, and X-ray analysis at 2.0 Å resolution of Val111Phe site-mutated calf chymosin. *Biochemistry* **1990**, *29*, 9863−9871.

(10) Newman, M.; Safro, M.; Frazao, C.; Khan, G.; Zdanov, A.; Tickle, I. J.; Blundell, T. L.; Andreeva, N. X-ray analyses of aspartic proteinases IV: structure and refinement at 2.2 Å resolution of bovine chymosin. *J. Mol. Biol.* **1991**, *221*, 1295−1309.

(11) Groves, M. R.; Dhanaraj, V.; Badasso, M.; Nugent, P.; Pitts, J. E.; Hoover, D. J.; Blundell, T. L. A 2.3 Å resolution structure of chymosin complexed with a reduced bond inhibitor shows that the active site β-hairpin flap is rearranged when compared with the native crystal structure. *Protein Eng.* **1998**, *11*, 833−840.

(12) Madala, P. K.; Tyndall, J. D. A.; Nall, T.; Fairlie, D. P. Update 1: Proteases universally recognize β strands in their active sites. *Chem. Rev.* **2010**, *110*, PR1−PR31.

(13) Metcalf, P.; Fusek, M. Two crystal structures of cathepsin D: the lysosomal targeting signal and active site. *EMBO J.* **1993**, *12*, 1293−1302.

(14) Davies, D. R. The structure and function of the aspartic proteinases. *Annu. Rev. Biophys. Biophys. Chem.* **1990**, *19*, 189−215.

(15) Robbins, A. H.; Dunn, B. M.; Agbandje-McKenna, M.; McKenna, R. Crystallographic evidence for noncoplanar catalytic aspartic acids in plasmepsin II resides in the Protein Data Bank. *Acta Crystallogr. D* **2009**, *65*, 294−296.

(16) Friedman, R.; Caflisch, A. On the orientation of the catalytic dyad in aspartic proteases. *Proteins* **2010**, *78*, 1575−1582.

(17) Pearl, L.; Blundell, T. The active site of aspartic proteinases. *FEBS Lett.* **1984**, *174*, 96−101.

(18) Chitpinityol, S.; Crabbe, M. J. C. Chymosin and aspartic proteinases. *Food Chem.* **1998**, *61*, 395−418.

(19) Dunn, B. M. Structure and mechanism of the pepsin-like family of aspartic peptidases. *Chem. Rev.* **2002**, *102*, 4431−4458.

(20) Coates, L.; Tuan, H.; Tomanicek, S.; Kovalevsky, A.; Mustyakimov, M.; Erskine, P.; Cooper, J. The catalytic mechanism of an aspartic proteinase explored with neutron and X-ray diffraction. *J. Am. Chem. Soc.* **2008**, *130*, 7235−7237.

(21) Farrell, H. M.; Jimenez-Flores, R.; Bleck, G. T.; Brown, E. M.; Butler, J. E.; Creamer, L. K.; Hicks, C. L.; Hollar, C. M.; Ng-Kwai-Hang, K. F.; Swaisgood, H. E. Nomenclature of the proteins of cows' milk − 6th revision. *J. Dairy Sci.* **2004**, *87*, 1641−1674.

(22) Brignon, G.; Chtourou, A.; Ribadeau-Duma, B. Preparation and amino acid sequence of human κ-casein. *FEBS Lett.* **1985**, *188*, 48−54.

(23) Nagy, K.; Váró, G.; Szalontai, B. κ-Casein terminates casein micelle build-up by its "soft" secondary structure. *Eur. Biophys. J.* **2012**, *41*, 959−968.

(24) Schechter, I.; Berger, A. On the size of the active site in proteases. I. Papain. *Biochem. Biophys. Res. Commun.* **1967**, *27*, 157−162.

(25) Palmer, D. S.; Christensen, A. U.; Sørensen, J.; Celik, L.; Qvist, K. B.; Schiøtt, B. Bovine chymosin: a computational study of recognition and binding of bovine κ-casein. *Biochemistry* **2010**, *49*, 2563−2573.

(26) Plowman, J. E.; Creamer, L. K. Restrained molecular dynamics study of the interaction between bovine κ-casein peptide 98−111 and bovine chymosin and porcine pepsin. *J. Dairy Res.* **1995**, *62*, 451−467.

(27) Srinivasan, J.; Cheatham, T. E., III; Cieplak, P.; Kollman, P. A.; Case, D. A. Continuum solvent studies of the stability of DNA, RNA, and phosphoramidate−DNA helices. *J. Am. Chem. Soc.* **1998**, *120*, 9401−9409.

(28) Christ, C. D.; Mark, A. E.; van Gunsteren, W. F. Feature article basic ingredients of free energy calculations: a review. *J. Comput. Chem.* **2010**, *31*, 1569−1582.

(29) Zwanzig, R. W. High-temperature equation of state by a perturbation method. 1. Nonpolar gases. *J. Chem. Phys.* **1954**, *22*, 1420−1426.

(30) Kirkwood, J. G. Statistical mechanics of fluid mixtures. *J. Chem. Phys.* **1935**, *3*, 300.

(31) Aqvist, J.; Medina, C.; Samuelsson, J. E. New method for predicting binding-affinity in computer-aided drug design. *Protein Eng.* **1994**, *7*, 385−391.

(32) Gohlke, H.; Case, D. A. Converging free energy estimates: MM-PB(GB)SA studies on the protein-protein complex Ras-Raf. *J. Comput. Chem.* **2004**, *25*, 238−250.

(33) Sørensen, J.; Hamelberg, D.; Schiøtt, B.; McCammon, J. A. Comparative MD analysis of the stability of transthyretin providing insight into the fibrillation mechanism. *Biopolymers* **2007**, *86*, 73−82.

(34) Kollman, P. A.; Massova, I.; Reyes, C.; Kuhn, B.; Huo, S.; Chong, L.; Lee, M.; Lee, T.; Duan, Y.; Wang, W.; Donini, O.; Cieplak, P.; Srinivasan, J.; Case, D. A.; Cheatham, T. E., III. Calculating structures and free energies of complex molecules: combining molecular mechanics and continuum models. *Acc. Chem. Res.* **2000**, *33*, 889−897.

(35) Gohlke, H.; Kiel, C.; Case, D. A. Insights into protein−protein binding by binding free energy calculation and free energy decomposition for the Ras−Raf and Ras−RalGDS complexes. *J. Mol. Biol.* **2003**, *330*, 891−913.

(36) Genheden, S.; Luchko, T.; Gusarov, S.; Kovalenko, A.; Ryde, U. An MM/3D-RISM approach for ligand binding affinities. *J. Phys. Chem. B* **2010**, *114*, 8505−8516.

(37) Swanson, J. M. J.; Henchman, R. H.; McCammon, J. A. Revisiting free energy calculations: a theoretical connection to MM/PBSA and direct calculation of the association free energy. *Biophys. J.* **2004**, *86*, 67−74.
(38) Miller, B. R.; McGee, T. D.; Swails, J. M.; Homeyer, N.; Gohlke, H.; Roitberg, A. E. MMPBSA.py: an efficient program for end-state free energy calculations. *J. Chem. Theory Comput.* **2012**, *8*, 3314−3321.
(39) Case, D. A.; Cheatham, T. E., III; Darden, T.; Gohlke, H.; Luo, R.; Merz, K. M., Jr.; Onufriev, A.; Simmerling, C.; Wang, B.; Woods, R. J. The Amber biomolecular simulation programs. *J. Comput. Chem.* **2005**, *26*, 1668−1688.
(40) Genheden, S.; Kuhn, O.; Mikulskis, P.; Hoffmann, D.; Ryde, U. The normal-mode entropy in the MM/GBSA method: effect of system truncation, buffer region, and dielectric constant. *J. Chem. Inf. Model.* **2012**, *52*, 2079−2088.
(41) The MathWorks Inc. Matlab R2011b, 2011,
(42) Massova, I.; Kollman, P. A. Computational alanine scanning to probe protein-protein interactions: a novel approach to evaluate binding free energies. *J. Am. Chem. Soc.* **1999**, *121*, 8133−8143.
(43) Huo, S.; Massova, I.; Kollman, P. A. Computational alanine scanning of the 1:1 human growth hormone-receptor complex. *J. Comput. Chem.* **2002**, *23*, 15−27.
(44) Moreira, I. S.; Fernandes, P. A.; Ramos, M. J. Computational alanine scanning mutagenesis − an improved methodological approach. *J. Comput. Chem.* **2007**, *28*, 644−654.
(45) Bradshaw, R. T.; Patel, B. H.; Tate, E. W.; Leatherbarrow, R. J.; Gould, I. R. Comparing experimental and computational alanine scanning techniques for probing a prototypical protein-protein interaction. *Protein Eng. Des. Sel.* **2011**, *24*, 197−207.
(46) Clackson, T.; Ultsch, M. H.; Wells, J. A.; de Vos, A. M. Structural and functional analysis of the 1:1 growth hormone:receptor complex reveals the molecular basis for receptor affinity. *J. Mol. Biol.* **1998**, *277*, 1111−1128.
(47) Farrell, H., Jr.; Wickham, E.; Dower, H.; Piotrowski, E.; Hoagland, P.; Cooke, P.; Groves, M. Characterization of the particles of purified κ-casein: trypsin as a probe of surface-accessible residues. *J. Protein Chem.* **1999**, *18*, 637−652.
(48) Møller, K. K.; Rattray, F. P.; Sørensen, J. C.; Ardö, Y. Comparison of the hydrolysis of bovine κ-casein by camel and bovine chymosin: a kinetic and specificity study. *J. Agric. Food Chem.* **2012**, *60*, 5454−5460.
(49) Vallejo, J. A.; Ageitos, J. M.; Poza, M.; Villa, T. G. Short communication: a comparative analysis of recombinant chymosins. *J. Dairy Sci.* **2012**, *95*, 609−613.
(50) Visser, S.; Van Rooijen, P. J.; Schattenkerk, C.; Kerling, K. E. Peptide substrates for chymosin (rennin). Kinetic studies with bovine κ-casein-(103−108)-hexapeptide analogues. *Biochim. Biophys. Acta* **1977**, *481*, 171−176.
(51) Visser, S.; Slangen, C. J.; van Rooijen, P. J. Peptide substrates for chymosin (rennin). Interaction sites in κ-casein-related sequences located outside the (103−108)-hexapeptide region that fits into the enzyme's active-site cleft. *Biochem. J.* **1987**, *244*, 553−558.
(52) Hill, R. D. The nature of the rennin-sensitive bond in casein and its possible relation to sensitive bonds in other proteins. *Biochem. Biophys. Res. Commun.* **1968**, *33*, 659−663.
(53) Hill, R. D. Synthetic peptide and ester substrates for rennin. *J. Dairy Res.* **1969**, *36*, 409−415.
(54) Dunn, B. M.; Jimenez, M.; Parten, B. F.; Valler, M. J.; Rolph, C. E.; Kay, J. A systematic series of synthetic chromophoric substrates for aspartic proteinases. *Biochem. J.* **1986**, *237*, 899−906.
(55) Dunn, B. M.; Valler, M. J.; Rolph, C. E.; Foundling, S. I.; Jimenez, M.; Kay, J. The pH dependence of the hydrolysis of chromogenic substrates of the type, Lys-Pro-Xaa-Yaa-Phe-(NO_2)Phe-Arg-Leu, by selected aspartic proteinases: evidence for specific interactions in subsites S3 and S2. *Biochim. Biophys. Acta* **1987**, *913*, 122−130.
(56) Fox, P. F.; Guinee, T. P.; Cogan, T. M.; McSweeney, P. L. H. Enzymatic coagulation of milk. In *Fundamentals of Cheese Science*; Fox, P. F., Guinee, T. P., Cogan, T. M., McSweeney, P. L. H., Eds.; Aspen Publishers: Gaitherburg, MD, 2000; pp 98−135.
(57) Andreeva, N.; Dill, J.; Gilliland, G. L. Can enzymes adopt a self-inhibited form? Results of x-ray crystallographic studies of chymosin. *Biochem. Biophys. Res. Commun.* **1992**, *184*, 1074−1081.
(58) Lee, A. Y.; Gulnik, S. V.; Erickson, J. W. Conformational switching in an aspartic proteinase. *Nat. Struct. Biol.* **1998**, *5*, 866−871.
(59) Humphrey, W.; Dalke, A.; Schulten, K. VMD: visual molecular dynamics. *J. Mol. Graphics Model.* **1996**, *14*, 33−38.